Mon. Not. R. Astron. Soc. **000**, 000–000 (0000) Printed 29 October 2015 (MN LATEX style file v2.2)

A Search for Correlations between Gamma-Ray Burst Variability and Afterglow Onset

S. A. Yost[1] and T. M. Moore
[1] *College of St. Benedict / St John's University, Collegeville, MN, 56321*
[2] *SGI, Eagan, MN, 55121*

arXiv:1510.08100v1 [astro-ph.HE] 27 Oct 2015

29 October 2015

ABSTRACT

We compared the time (or time limit) of onset for optical afterglow emission to the γ-ray variability V in 76 GRBs with redshifts. In the subset (25 cases) with the rise evident in the data, we fit the shape of the onset peak as well and compared the rising and decaying indices to V. We did not find any evidence for any patterns between these properties and there is no statistical support for any correlations. This indicates a lack of connection between irregularities of the prompt γ-ray emission and the establishment of the afterglow phase. In the ordinary prompt internal shocks interpretation, this would indicate a lack of relationship between V and the bulk Lorentz factor of the event.

Key words: gamma-ray: bursts

1 INTRODUCTION

Gamma-ray bursts (GRBs) are the most luminous explosions in the universe. The γ-ray dominated prompt emission typically lasts from a fraction of a second to tens of seconds, followed by lower-energy, longer-lasting afterglow. These events are interesting because they are extreme; they require highly relativistic outflows and are associated with the deaths of massive stars or the merger of compact remnants. GRBs can also probe the environment in distant galaxies since the material swept up by the event's external shock drives the afterglow.

Mészáros (2006) gives an exhaustive review of observations and theory as of a few years ago. The broad features of afterglow emission are well described by synchrotron radiation from relativistic electrons swept up by a self-similar external shock, even though the details of the shock such as its microphysics are not always clear. GRB prompt emission is highly irregular compared to the afterglow. Even the prompt radiation mechanism is poorly understood, with models that include internal shocks in the relativistic outflow with synchrotron, inverse Compton radiation or "jitter" radiation, as well as magnetic reconnection to dissipate energy, or even radiation from the relativistic hadrons. Gehrels & Razzaque (2013) and Mészáros & Gehrels (2012) are recent reviews with more details about theoretical models, including these prompt emission models, in light of ongoing progress from *Swift* and *Fermi* results.

The prompt mechanisms produce great case-by-case variations in γ-ray light-curves, from single pulses to very irregular multi-peaked cases or events with pauses between γ-ray activity. There are also different possibilities for the start of the afterglow, with some initiated during the prompt emission, others delayed until after the high-energy light has ceased, and some showing flares or rebrightening. These effects are not just observed in the X-rays which would have some of the end of the prompt emission as well as afterglow light, but are all seen in optical light (discussed in reviews and notable in compilations of afterglow light-curves such as Roming et al. (2009); Rykoff et al. (2009)).

Despite many efforts to categorize or correlate prompt γ-ray properties with other information (e.g., reviewed in the parameter correlation section of Kumar & Zhang 2015), there have been few results compared to the understanding offered by afterglows. One area in which a prompt properties could shed light on the afterglow, however, is this range in afterglow onset characteristics. Even the simplest theoretical examination of GRBs expected more than one type of afterglow onset, depending upon properties that would also relate to prompt emission. Sari & Piran (1999) noted two regimes of thickness for a relativistic shell whose internal shocks produce the prompt GRB. The division between "thick" and "thin" depended not only on the shell's physical thickness but also its Lorentz factor. Thin shells were expected to finish emitting prompt radiation before sweeping up enough material to become self-similar and show afterglow while thick shells would have the same timescale to complete the internal shocks (end the GRB) and initiate the afterglow. This would be observed as a rise, or as the end of of dominance by rapidly-decaying reverse shock radiation.

This simple picture does not explain the observed early

afterglows, which includes events with established afterglows during the prompt GRB. As seen in afterglow compilations, few events show the characteristic rapidly-declining reverse shock before the slowly-declining synchrotron afterglow. Many events have decaying afterglows during the γ-ray emission which cannot be attributed to the reverse shock; the rise may be seen or the decay is shallow and continues to late times. Onsets after the GRB have varied optical delays, and may indicate that the events (usually "long" bursts) are "thin" shell cases (e.g. as applied by Molinari et al. 2007) and the delay time indicates the initial Lorentz factor of the event in a manner that is only weakly dependent on other factors like the kinetic energy or circumburst density (noted in Sari & Piran 1999). However, there are also other models for the delays, such as the effects of off-axis viewing of the relativistic outflow (Panaitescu et al. 2013). Moreover, the models are incomplete in other ways. Some events have observed onsets which are so steep that it is difficult for any model to account for the rapid rise in optical flux (e.g. GRB110205A, where Cucchiara et al. 2011, examined the afterglow for forward and reverse shock onset behaviour and could only match the event to one model by changing the reference time for the start of emission).

The range in delays before the self-similar optical afterglow phase continues to be poorly understood. The properties of the afterglow onset have been investigated to compare it to afterglow models, both within the optical itself and between the early optical and X-ray light-curves (with a great deal of work by Liang et al. 2010, 2013). Liang et al. (2013) has also systematically compared the optical onset lightcurve's peak properties to those of any late optical rebrightening "bump" and the event's γ-ray energy properties. They found correlations between optical properties of the onset peak, and between the optical peak luminosity and the total γ-ray energy.

This work probes whether there is any connection between measures of optical afterglow onset properties and the "variability measure" (V) of the prompt GRB. Variability is defined as the normalized squared difference between a GRB light-curve and an appropriately-smoothed version of the light-curve. It should quantify how irregular, spiky, multi-peaked, etc. a burst is. The diversity in this property is obvious among GRB light-curves (noted from early on, e.g., Fishman & Meegan 1995), and must connect to some variable physical property that results in irregularity in the prompt emission process(es).

The variability may also be related to the luminosity of the prompt γ-rays, e.g. as studied by Reichart et al. (2001), Schaefer (2007), Xiao & Schaefer (2009) and others. The irregularity in prompt energy production and emission processes (or the luminosity) could connect to how the event establishes the external shock. Therefore it is particularly interesting whether V connects to the initial optical peak time which should indicate the start of the afterglow phase.

Another possible connection involves afterglow onset delays after the end of a GRB. If this does indicate that the event has a "thin" shell, the timing is mostly dependent upon the initial Lorentz factor. Then a connection between variability and onset time would indicate a connection between the overall speed of the relativistic outflow and its irregularity. If the observed onset delays are due to another cause like off-axis viewing angles, any connection to V would indicate that the outflow properties related to irregular prompt processes could vary with the off-axis angle of the flow.

A connection between γ-ray properties and delays in cases where the afterglow onset is before the end of the GRB is also interesting. This is due to afterglow onsets during a GRB not being expected in the simple GRB picture. Sari & Piran (1999) find that in the internal-external shock model, most of the energy of a "thick" shell is extracted to start the afterglow at approximately the time it takes to complete the internal shock phase. This is found with simple scalings rather than examining details of how prompt emission might affect the developing external shock. In the case where the afterglow is established during the GRB itself, if the timing is connected to V then it would indicate that highly irregular prompt processes enhance or inhibit the start of the afterglow. This would be a clue to where the simple picture breaks down.

2 METHODS

We selected a set of GRBs with early observations, complete through early 2012. The definition of "early" observations required either a report of a rising optical light-curve, or a detection with some indication of fading behaviour in the first 20 minutes (just over 1 ksec) after the trigger. The set only included those with a redshift measurement, as z has a slight effect on the calculation of V and it is essential to compare items in the GRB emission frame. The set was further limited to *Swift*-detected GRBs, as their γ-ray light-curves and background are consistently available. Finally, a GRB needed a duration measure to be included. We use the T_{90} as a proxy. This is the time to observe 90% of the fluence above the background starting from when 5% has been observed, a measure that is nearly always available.[1] The final set of 76 events is included with its V calculations in Table 1.

2.1 Gamma-Ray Variability V

There are many ways to implement the basic description of V, especially when attempting to decide what the appropriate smoothing timescale would be and how to minimize dependences on redshift or burst spectral shape (which may not be measurable) or biases from observer effects like time bins. For GRBs, this has led to several different measures (e.g. Fenimore & Ramirez-Ruiz 2000; Reichart et al. 2001; Schaefer 2007). We use the variability equations from Reichart et al. (2001), which takes a smoothing timescale definition that isn't biased by precursors or episodes of low counts.

Reichart et al. (2001) includes two variability measurements, the comparison between the data and the smoothed light-curve ("V_1", the paper's equation 5) and one which approximates the removal of Poisson noise effects on the variability ("V_2", the paper's equation 7). V_2 is theoretically

[1] Rare exceptions when spacecraft pointing prevented a clear view of the end of a GRB produce T_{90} limits, such as GRB080319B, which was not considered.

a better measure of GRB γ-ray properties, but its use had problems. V_1 is reported as V in table 1 and used for variabilities. Values of V_2 were also used in the analyses, with no difference in the conclusions.

These problems with V_2 may be due to the need to estimate the background as constant, as described below. V_2 broadly tracked V_1 except for 7 cases where V_1 was at the large end and the estimated uncertainty in V_2 (equation 8 in the paper) was greater than 1 variability unit (although this was still only about a 10% uncertainty). Results with V_1 did not change when these 7 events were excluded. In 2 of these cases, the denominator for V_2 was negative, giving a negative variability value. The denominator is more dependent on the background values than the numerator; this may indicate a significant inaccuracy approximating Poisson noise effects with an approximate, constant background level.

V calculations implement a smoothing timescale that varies between events, using a time required for the detection of a fraction of the fluence. The fraction $f = 0.45$ was adopted since that had been used with reasonable results in Reichart et al. (2001).

The calculations require a time range that includes the complete event, which can be difficult to determine precisely with the noise relative to background. Since the light-curves are of various durations, we calculated V using data that is expected to include the entire GRB time by taking extra time before and after the reported GRB duration. The most common duration measure, T_{90}, by design does not include the entire GRB. Rather than use ad hoc times by inspection, we calculated all the measures based on the T_{90} plus a fraction of T_{90} before the trigger and after the end of T_{90}. The time range used for the reported values is "$T_{90} \pm 30\%$". However, we also ran "$\pm\,10\%$" and "$\pm\,50\%$" cases, with no change to our conclusions[2].

The equations require the total and background counts in each time bin, which were obtained as a background level and the background-subtracted light-curves for the full energy band (15–350 keV). The *Swift* background-subtracted light-curves are available as text files from the ground-analysis site[3]. These are in units of counts s^{-1} cm^{-2} and are converted to counts using the 64-ms bin size and the *Swift* 1400 cm^2 effective area[4]. The γ-ray background level was found in the TDRSS records[5] which include non-background-subtracted images of the light-curves in nearly all cases[6] The background was then approximated as constant throughout the GRB event and its value was found by inspection of the event's images. The units were also counts s^{-1} and converted to counts in a 64-ms bin. The background level was added to the light-curve for the total counts in the calculations.

We verified that changing the assumed background level by 3–5% had no appreciable effect on the variability calculation. This was a reasonable estimate of our ability to determine a background level from the TDRSS images (a difference of 200–400 in a typical level of 7500 counts s^{-1}, which is a noticeable change on the plot axis). Specifically, we noted whether the results changed relative to the only uncertainty calculation available. This is δV the estimated uncertainty in "V_2". When we changed the background by $\pm 3\%$, the values of V changed by $< \delta V$ in 70% of cases and by $< 2\,\delta V$ in 97% of cases. When the background changed by 5%, the changes in V were still not extreme by comparison with the estimated uncertainty: 82% changed by $< 2\,\delta V$ and 96% by $< 3\,\delta V$.

[2] Some values of V increased with the increasing time range, but this did not affect our analysis of correlation evidence.
[3] BAT TXT links at http://gcn.gsfc.nasa.gov/swift_gnd_ana.html
[4] see http://swift.gsfc.nasa.gov/analysis/bat_digest.html
[5] BAT TLC links at http://gcn.gsfc.nasa.gov/swift_gnd_ana.html
[6] Events 050319, 050401, 060927, 070721B, 080906, and 120119A were eliminated as the non-background-subtracted light-curves were not available.

2.2 Optical Properties

Most optical peak time limits came from initial decays evident in light-curves from journal articles or GCN notices; Table 2 references the data sources. Usually a trend of many points is noted. In cases of sparse early data we required that two successive points in the same filter show an initial decay. If the initial points were separated by a long time baseline (a factor > 2) they were not considered a reliable indication of decay since a sharp rise and rollover can occur on that logarithmic timescale; a subsequent pair (e.g., the second and third points) that were more closely-spaced and showed an early decay would set the peak limit time. In a few cases no early light-curve points are published but there is a GCN message indicating an initial decay which then sets the peak time limit for the event.

Cases with an observed rise were fitted to an onset peak shape function, as done by Liang et al. (2010) (their equation 1). The full onset through the initial decay is used except in some cases with very long data gaps or where part of the decaying light-curve was excluded due to signs of further flaring / rebrightening. Rather than trying to determine what constitutes a flare to censor a small part of the light-curve, the dataset is cut off, as noted in Table 3. Not all of the events fit well statistically to the formula, but the fits did describe the trend of the onset data; see Figures 1, 2. The results are in Table 3, along with information about each data source. This includes events 080804 and 110801a, whose full datasets were not published and were obtained directly from the ROTSE-III project (Akerlof, priv. comm.).

We noted three cases with appropriate γ-ray data, z, and optical peak information which did not easily match the "decaying gives a peak limit" or "rising / falling allows on onset fit" cases. These are GRBs 070411, 100418A and 100901A. The light-curves are plotted in Figure 3, showing fairly flat initial light-curves. We considered three ways to interpret these events: (1) exclude them (2) take the onset or peak as the point when the optical rise is complete or (3) take the onset or peak as the point where the decay has begun. Table 4 discusses the values for options (2) and (3). We performed calculations for all three methods and the exclusion or inclusion method did not affect the results. The results and calculations presented in this paper simply exclude these three events.

2.3 Checking for Correlations

While the optical onset time could have a relationship to the γ-ray properties, it was also interesting to examine any onset

properties including the onset peak shape parameters. There have been some cases of unexpected early afterglow rise and decay rates (discussed in section 6 of Mészáros 2006). There are no theories directly expecting the γ-ray variability to cause these effects, but any correlation could provide a clue to the unusual cases.

An initial examination versus V showed no evident patterns (see Figures 4–8). The rise-to-decay index ratio r/d might have a loose positive correlation with V. Peak times were examined both de-redshifted ($T_{pk}/(1+z)$) and as a fraction of the GRB duration proxy T_{90} (T_{pk}/T_{90}). The points for the peak times suggest a loose correlation with V. The peak limits, however, do fill in much of the parameter space.

The relationships were then investigated quantitatively via correlation tests using a Spearman rank coefficient ρ, as implemented by the Iraf STSDAS package. This calculation permits censored points (limits like the peak times) but does not use uncertainty information.

The Spearman results are in Table 5. For 20 cases of optical peak fits, the indices r and d were constrained (reported uncertainty $< 1/3$ of the fitted value), allowing comparisons of V to each index and the ratio r/d (a proxy for asymmetry). These are fewer than the threshold of 30 data points for a reliable Spearman correlation test; the results are included to show that there are no statistically obvious correlations which could be hinted at by the results with 20 points. The fitted peak flux density is not considered, as the comparison between events would require accounting for poorly-constrained local extinction along with very careful adjustments for different filters and redshifts.

3 RESULTS & DISCUSSION

Figures 4 and 5 show the variation of peak times (de-redshifted and as a fraction of the GRB duration) versus variability; the points show the uncertainties reported from the fits. With some irregular instead of smooth behaviour, not all the fits are statistically good as shown by the χ^2 in Table 3. However, figures 1 and 2 demonstrate that the fits match the peak times and overall shapes. While the peak time points suggested a trend, the Spearman coefficients show null (no correlation) probabilities of 1.6% for the source frame peak times and 2.0% for the times as a fraction of the duration T_{90}. These confidence levels for a correlation would correspond to 2.4 σ and 2.3 σ in a normal distribution.

Figures 6–8 show the indices and rising/falling index ratio versus variability. The plots of the decaying index and the ratio r/d suggest a broad relationship, but again there is no statistical support for it. The null probabilities are 0.9% for r, 45% for d and 1.6% for r/d, or no better than confidence levels equivalent to 2.6, 0.8, or 2.4 σ in a normal distribution.

As previously discussed, there are uncertainties in the treatment of the data (three hard-to-classify cases, other time bases, etc). Some of these provide even larger null probabilities for correlations. Moreover the Spearman test does not take uncertainties into account. These factors tend to lessen any confidence in the slight (and not statistically significant) confidence levels for a correlation. There is therefore no statistically compelling support for a connection between the variability of the prompt GRB emission and the afterglow onset properties, particularly the optical rise times.

Table 1: GRBs and their Variability Measures

GRB	$T_{90}\,(s)$	z	V	z Reference
050502A	58.9	3.793	1.5	Prochaska et al. (2005b)
050525A	8.8	0.606	2.0	Foley et al. (2005)
050730	156.5	3.969	7.8	Prochaska et al. (2005a)
050802	19	1.71	1.2	Fynbo et al. (2005)
050820A	26	2.615	3.4	Ledoux et al. (2005)
050908	19.4	3.35	3.3	Fugazza et al. (2005)
050922C	4.5	2.198	0.057	Jakobsson et al. (2005)
051109A	37.2	2.346	0.60	Quimby et al. (2005)
051111	46.1	1.549	0.61	Prochaska (2005)
060108	14.3	2.03	3.1	Melandri et al. (2006a)
060206	7.6	4.045	0.22	Fynbo et al. (2006a)
060418	103.1	1.49	0.54	Prochaska et al. (2006)
060502A	28.4	1.51	0.083	Cucchiara et al. (2006)
060510B	275.2	4.9	8.0	Price (2006)
060512	8.5	0.4428	2.6	Bloom et al. (2006)
060605	79.1	3.8	3.9	Peterson & Schmidt (2006)
060607A	102.2	3.082	2.2	Ledoux et al. (2006)
060904B	171.5	0.703	1.2	Fugazza et al. (2006)
060908	19.3	1.884	0.55	Fynbo et al. (2009)
060912	5	0.937	0.061	Jakobsson et al. (2006)
060926	8	3.208	2.0	D'Elia et al. (2006)
061007	75.3	1.261	0.14	Osip et al. (2006)
061110A	40.7	0.758	6.7	Fynbo et al. (2007)
061110B	134	3.44	2.4	Fynbo et al. (2006b)
070318	74.6	0.836	2.0	Jaunsen et al. (2007)
070411	121.5	2.954	7.3	Jakobsson et al. (2007)
070419A	115.6	0.97	5.9	Cenko et al. (2007b)
071003	150	1.1	6.0	Perley et al. (2007)
071010A	6	0.98	2.3	Prochaska et al. (2007)
071010B	35.7	0.947	0.086	Cenko et al. (2007a)
071020	4.2	2.142	0.10	Fatkhullin et al. (2007)
071031	180	2.692	3.9	Ledoux et al. (2007)
080210	45	2.641	1.7	Jakobsson et al. (2008b)
080319C	34	1.95	0.32	Wiersema et al. (2008)
080330	61	1.51	2.3	Malesani et al. (2008)
080413A	46	2.433	0.50	Thoene et al. (2008b)
080413B	8	1.10	0.027	Vreeswijk et al. (2008)
080430	16.2	0.767	0.77	Cucchiara & Fox (2008)
080603B	60	2.69	0.54	Fynbo et al. (2008a)
080605	20	1.64	0.13	Jakobsson et al. (2008c)
080607	79	3.036	0.11	Prochaska et al. (2008b)
080710	120	0.845	1.5	Perley et al. (2008a)
080721	16.2	2.602	0.14	D'Avanzo et al. (2008)
080804	34	2.2045	0.53	Thoene et al. (2008a)
080805	78	1.505	2.1	Jakobsson et al. (2008a)
080810	106	3.35	1.5	Prochaska et al. (2008a)
080913A	8	6.7	1.5	Fynbo et al. (2008b)
081029	270	3.848	3.0	D'Elia et al. (2008)
081203A	294	2.1	1.1	Landsman et al. (2008)
081222	24	2.77	0.059	Cucchiara et al. (2008)
090102	27	1.547	0.36	de Ugarte Postigo et al. (2009b)
090313	79	3.375	1.5	Chornock et al. (2009c)
090424	48	0.544	0.12	Chornock et al. (2009b)
090426	1.2	2.609	0.13	Levesque et al. (2009)
090618	113.2	0.54	0.10	Cenko et al. (2009)
090715B	266	3.00	0.68	Wiersema et al. (2009)
090726	67	2.71	3.1	Fatkhullin et al. (2009)
090812	66.7	2.452	0.66	de Ugarte Postigo et al. (2009a)
091018	4.4	0.971	0.046	Chen et al. (2009)

091024	109.8	1.092	1.2	Cucchiara et al. (2009)
091029	39.2	2.752	0.93	Chornock et al. (2009d)
100316B	3.8	1.180	1.3	Vergani et al. (2010)
100418A	7	0.6235	1.8	Antonelli et al. (2010)
100621A	63.6	0.542	0.10	Milvang-Jensen et al. (2010)
100728A	198.5	1.567	0.66	Kruehler et al. (2013)
100814A	174.5	1.44	1.1	O'Meara et al. (2010)
100816A	2.9	0.8034	0.027	Tanvir et al. (2010)
100901A	439	1.408	1.8	Chornock et al. (2010)
110128A	30.7	2.339	2.3	Sparre et al. (2011)
110422A	25.9	1.77	0.047	Malesani et al. (2011)
110503A	10	1.613	0.038	de Ugarte Postigo et al. (2011)
110801A	385	1.858	2.0	Cabrera Lavers et al. (2011)
111107A	26.6	2.893	1.5	Chornock et al. (2011)
111228A	101.2	0.7163	0.34	Schulze et al. (2011)
120326A	69.6	1.798	0.16	Tello et al. (2012)
120327A	62.9	2.813	0.86	Sanchez-Ramirez et al. (2012)

GRB events used are presented with their observed 90% γ-ray duration T_{90} (from the *Swift* archive) and their redshift. Variability V examines the irregularity of the γ-rays by comparing the GRB lightcurve relative to itself smoothed by a time corresponding to observing 45% of the fluence. The variability is the first measure discussed in Reichart et al. (2001). As noted, there were problems with the second measure which approximately accounts for removing Poisson noise variability effects from this calculation. The results presented use $T_{90} \pm 30\%$ to get a background region. Variabilities were also calculated using $\pm\,10\%$ and $\pm\,50\%$. Some numbers changed between background selection regions by more than the estimated variability uncertainty, which is actually the $\delta\,V$ estimate for the closely-related second variability measure of Reichart et al. (2001). However, the overall conclusions about the lack of evidence for correlations did not.

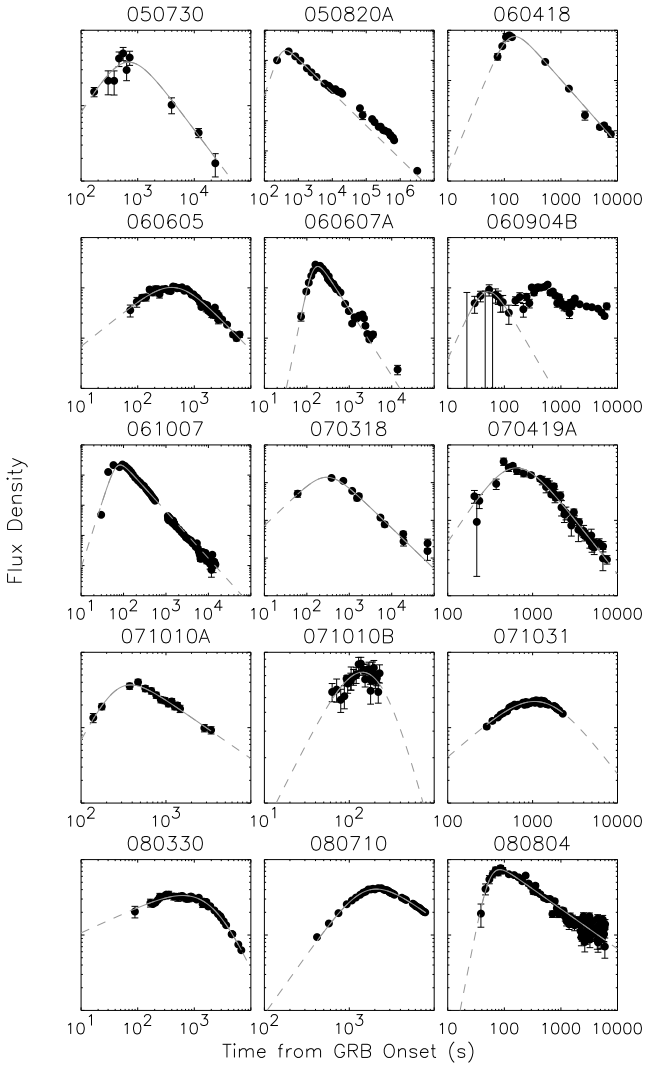

Figure 1. Fits to the cases with evidence of a rising peak, part 1. Fit results and data references are in Table 3. Later times are excluded in some cases to avoid flares, rebrightenings, steepening decay, or data gaps; these parts are shown in dashed lines for the fit model. The fits give a good representation of the shape even in cases with poor χ^2, and so are useful for determining the peak times for further analysis

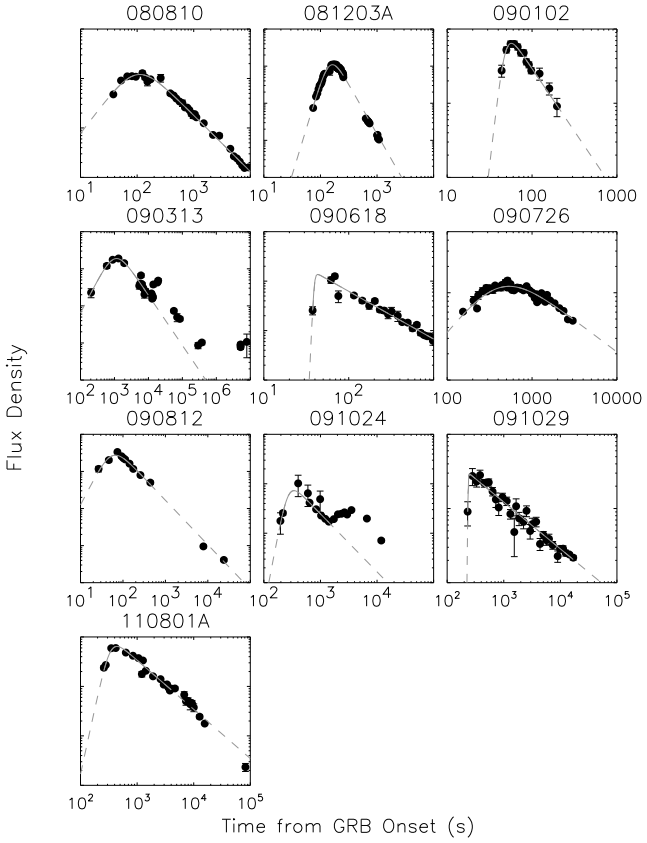

Figure 2. Fits to the cases with evidence of a rising peak, part 2. See Figure 1 for details.

This lack of relationship between the variability V of the prompt GRB and the time it takes to establish the afterglow implies a lack of connection between V and the "thick" versus "thin" outflow cases of the prompt internal shock model, or the off-axis line of sight or dust destruction timescales in other onset models referred to in the introduction. As noted, the delay is commonly interpreted as indicating the outflow Lorentz factor of a "thin" shell. In that case, our result suggests that there would be no strong connection between how variable the GRB outflow is and its overall Lorentz factor.

Other groups have studied the variability of the prompt GRB for any connection to the γ-ray luminosity, as a luminosity indicator would be an important tool in cosmological studies (e.g. Reichart et al. 2001; Schaefer 2007; Xiao & Schaefer 2009). However, Xiao & Schaefer (2009) analyzed several prompt GRB properties and noted that V is their "most noisy" luminosity relation, compared to properties that included spectral information or energetics; they did not study V as a luminosity indicator in that work. Variability may not be an indicator of the prompt luminosity, yet if it is then our work implies that there is no strong association between the luminosity of the prompt event and the properties of the afterglow onset.

4 CONCLUSIONS

We compared the optical afterglow onset times (or limits) to the γ-ray variability V in 76 GRBs with redshifts. In a subset of 25 cases, we fit the shape of the onset "bump" as well and compared the rising and decaying indices to V. We did not find any evidence for a pattern and there is no statistical support for any correlations. This indicates a lack of connection between irregularities of the prompt γ-ray emission and the establishment of the afterglow phase. In the ordinary prompt internal shocks interpretation, this would indicate a lack of relationship between V and the bulk Lorentz factor of the event.

ACKNOWLEDGEMENTS

We acknowledge the use of public data from the *Swift* data archive

We acknowledge the use of data from the ROTSE-III project. The ROTSE project was made possible by grants from NASA, NSF, and the Australian Research Council, and

Table 2. Optical Peak Time Upper Limits

GRB	T_{PK} Limit (s)	Data Source
050502A	68.95	Yost et al. (2006)
050525A	66	Rykoff et al. (2009)
050802	286	Oates et al. (2007)
050908	377	de Pasquale et al. (2005)
050922C	174.9	Rykoff et al. (2009)
051109A	37.9	Rykoff et al. (2009)
051111	29.4	Yost et al. (2007)
060108	532	Oates et al. (2006)
060206	319	Monfardini et al. (2006)
060502A	134	Poole & La Parola (2006)
060510B	168	Melandri et al. (2006b)
060512	99	de Pasquale & Cummings (2006)
060908	88	Oates et al. (2009)
060912	114	Oates et al. (2009)
060926	91	Lipunov et al. (2006b,a)
061110A	76	Zhai et al. (2006)
061110B	1200	Melandri et al. (2006c)
071003	44.5	Perley et al. (2008b)
071020	25.6	Schaefer et al. (2007); Yuan et al. (2007)
080210	345.9	Klotz et al. (2008a)
080319C	47.6	Wren et al. (2008)
080413A	22.9	Rykoff & Rujopakarn (2008)
080413B	76.5	Filgas et al. (2011)
080430	18.8	Klotz et al. (2008b)
080603B	25.4	Rujopakarn et al. (2008)
080605	414	Kann et al. (2008)
080607	24.5	Perley et al. (2011)
080721	423	Starling et al. (2009)
080805	558	de Ugarte Postigo et al. (2008)
080913A	576	Greiner et al. (2009)
081029	88.5	Holland et al. (2011)
081222	28	Covino et al. (2008a)
090424	87	Xin et al. (2009)
090426	86	Xin et al. (2011)
090715B	648	Guidorzi et al. (2009a)
091018	405.6	Wiersema et al. (2012)
100316B	34	Haislip et al. (2010)
100621A	240	Updike et al. (2010)
100728A	47	Perley et al. (2010)
100814A	278	Saxton et al. (2010)
100816A	595.7	Oates et al. (2010)
110128A	126.2	Laas-Bourez et al. (2011)
110422A	58.7	Gorbovskoy et al. (2013)
110503A	212	Oates (2011)
111107A	885	Lacluyze et al. (2011b,a)
111228A	254.1	Krushinski et al. (2011)
120326A	163	Klotz et al. (2012b,a)
120327A	864	Meehan et al. (2012)

Subsample with early optical or near-IR decays giving limits on the optical peak time, and so the onset of the optical afterglow. Initial decays were noted within 20 minutes of the trigger, thus some optical emission has already risen regardless of subsequent flares or rebrightening. Many references are from GCN Notices. Usually a trend of several points indicates the decay. Sparse early data required two consecutive points showing decay in the same filter, separated in time by no more than a factor of 2 to avoid the possibility of missing a sharp peak. Cases where the first two points were too far apart in time used later points to set the limit, e.g., the second & third. In a few cases, a single GCN Notice indicates one point but declares that the transient is fading, which is taken as sufficient confirmation for the limit. As can be seen in Figures 4 and 5, these limits fill in part of peak time–variability plot, while the detections alone make these appear to be loosely correlated.

Table 3. Optical Initial Peak Fits

GRB	T_{PK} (s)	δT_{PK} (s)	r	δr	d	δd	χ^2 / DOF	Avoiding flares/dips	Data source
050730	690	150	1.19	0.21	1.00	0.07	6.7 / 6		1
050820A	422	12	3.38	0.34	1.10	0.02	17.6 / 4	$t \leq$ 7ks	2
060418	153.3	3.3	2.70	0.22	1.27	0.02	15.8 / 8		3
060605	399	12	0.90	0.09	1.17	0.05	74.5 / 50		4
060607A	180.9	2.4	4.15	0.22	1.32	0.04	45.7 / 23	$t \leq$ 1ks	3
060904B	52.1	8.9	2.51	2.48	1.94	2.15	2.2 / 7	$t \leq$ 130s	4
061007	83.39	0.45	4.39	0.05	1.56	0.01	2377 / 19	$t \leq$ 600s	4
070318	295	21	1.09	0.14	1.08	0.05	17.2 / 8		5
070419A	643	20	1.70	0.19	1.44	0.05	47.5 / 42	$t \leq$ 10ks	6
071010A	384	22	2.13	0.20	0.78	0.05	4.8 / 12	$t \leq$ 3.6ks	7
071010B	143	12	1.13	0.69	2.17	5.41	17.2 / 24		8
071031	1057	29	0.98	0.05	1.48	0.19	29.4 / 39	$t \leq$ 2.3ks	9
080330	622	16	0.34	0.02	1.77	0.11	30.1 / 36	$t \leq$ 10ks	10
080710	2090.6	4.9	1.59	0.01	0.820	0.005	596 / 36	$t \leq$ 8ks	11
080804	83.3	3.9	3.84	0.69	0.53	0.01	173 / 85		0
080810	111.4	1.4	1.50	0.05	1.14	0.01	132 / 28		12
081203	163.42	0.26	4.99	0.02	2.68	0.04	1037 / 42	$t \leq$ 400s	13.
090102	57.0	1.5	9.88	2.35	1.69	0.18	4.9 / 9		14
090313	1154	91	1.76	0.24	1.35	0.14	19.3 / 8		15
090618	45.47	0.41	24.53	8.78	0.96	0.03	26.9 / 18	$t \leq$ 1ks	0
090726	538	11	1.21	0.05	0.73	0.03	198 / 43		16, 17
090812	66.3	4.0	2.21	0.49	1.20	0.12	9.7 / 6	$t \leq$ 1ks	18
091024	340	76.4	6.00	5.57	1.17	0.06	3.8[a] / 6	$t \leq$ 1.5ks	19–24,
091029	267.2	4.3	30.82[b]	0.55	0.63	0.02	34.7 / 27		25
110801A	439.9	8.2	5.25	0.38	0.99	0.02	105 / 14	$t \leq$ 4ks	0, 26–28

Subsample with an initial rise, fitted to an empirical shape with rising / decaying asymptotic powerlaw indices r and d, the peak time T_{pk}, and the peak flux density. The peak flux density is not considered for further analysis, as this would require corrections for poorly-known local extinction, so the results are not reported. In some cases later parts of the available data have been excluded from the fits to avoid flares, rebrightening, steepening after the initial decay, or a data gap in the decay; these are noted in the column "Avoiding flares / dips". The fits are all plotted in Figures 1 and 2, with dashed lines for any part of the time range which was excluded from the fit. Except for 061007's extremely sharp rise, the fits give a good overall match to the shape of the onset even when the χ^2 is large. The formal uncertainties on the parameters may not account for the full uncertainty when the fit is not good, and the formal uncertainties show that r and d are unconstrained in some cases. In such cases, T_{pk} is useful for correlation analysis but r and d are not.

0. *Akerlof, priv. comm.*; 1. Blustin et al. (2005); 2. Cenko et al. (2010); 3. Molinari et al. (2007); 4. Rykoff et al. (2009); 5. Roming et al. (2009); 6. Melandri et al. (2009); 7. Covino et al. (2008b); 8. Wang et al. (2008); 9. Krühler et al. (2009b); 10. Guidorzi et al. (2009b); 11. Krühler et al. (2009a); 12. Page et al. (2009); 13. Kuin et al. (2009); 14. Klotz et al. (2009); 15. Melandri et al. (2010); 16 Maticic & Skvarc (2009); 17 Šimon et al. (2010); 18. Dado & Dar (2009); 19. Gruber et al. (2011); 20. Mundell et al. (2009); 21. Cano et al. (2009); 22. Henden et al. (2009); 23. Updike et al. (2009); 24.Chornock et al. (2009a); 25. Lacluyze et al. (2009);26. Sokolov et al. (2011); 27. Parhomenko et al. (2011); 28. Kuroda et al. (2011);

[a] 4 early GCN points with no uncertainties were employed with 0.5-magnitude uncertainties

[b] The first two points show a steep rise, but this index r is inconsistent with the index found in the i band, casting doubt on the optical onset shape fit. This event was not used in tests for r and d correlations

through participation and support from the University of Michigan, Los Alamos National Laboratory, and the University of New South Wales.

STSDAS is a product of the Space Telescope Science Institute, which is operated by AURA for NASA

REFERENCES

Antonelli L. A. et al., 2010, GRB Coordinates Network, 10620, 1

Bloom J. S., Foley R. J., Koceveki D., Perley D., 2006, GRB Coordinates Network, 5217, 1

Blustin A. J., Holland S. T., Cucchiara A., White N., Hinshaw D., 2005, GRB Coordinates Network, 3717, 1

Cabrera Lavers A., de Ugarte Postigo A., Castro-Tirado

Table 4. Optical Rise / Peak Special Cases

GRB	T_{PK} (s) established by rise	T_{PK} (s) established by decay	data source
070411	250 ± 30	< 800	Ferrero et al. (2008)
100418A	< 162	$< 5 \times 10^4$	Marshall et al. (2011)
100901A	< 153.4	1800 ± 600	Gorbovskoy et al. (2012)

Three events with marginal evidence of a rise, or an apparent plateau. They are shown in Figure 3; 070411's data is adapted from Figure 2 of Marshall et al. (2011), but does not show the time error bars. The events are treated 3 different ways for the search for correlations between γ-ray variability and the optical onset. They are given a peak value or limit consistent with "onset" being at the end of an optical rise (limited by being before a plateau), before the beginning of a decay (conservatively limited by the end of a plateau), or excluded from the analysis. 070411 is assigned a peak value instead of a limit for the first case, due to the discussion of a rising phase in Marshall et al. (2011); the uncertainty comes from the duration of the second light-curve point. 100901A is assigned a peak value for the second case as the optical peak fit was attemped through the clear decay after 1 hour. The results were not constrained and are not in Table 3, but this gives a good estimate of the start of the decay.

Table 5. Spearman Correlation Coefficient Results

Item Compared	Spearman ρ	Null Probability
T_{pk}/T_{90} (1)	0.274	0.0201
$T_{pk}/(1+z)$ (1)	0.299	0.0159
Correlation Tests for Optical Onset Peak Shape (Indices)		
N=20 cases, test not considered accurate for N < 30		
r	-0.603	0.0086
d	-0.173	0.4510
r/d	-0.553	0.0159

Correlation test results. Variability tested with the peak time includes the limits but excludes the 3 hard-to-classify cases (Figure 3). The peak correlation tests use 73 events and do not support a relationship between the variability and the optical onset time either de-redshifted or as a fraction of the duration T_{90}. The 3 hard-to-classify cases were also considered by including their peak time as set by the rise as well as the peak time as set by the decay (see Table 4); neither case changed the results. Correlation tests for the peak shape (rising index r, decaying index d, and their ratio) are included to show that they do not suggest a correlation. Only events with a fitted initial peak where the formal relative uncertainties of indices were $< 1/3$ could be considered constrained and their values used. The correlation tests for the indices are not considered accurate due to the small number of available points. As noted, we considered a background region of 30% of T_{90} when calculating the variability. We also performed correlation tests with the variabilities calculated using background regions of 10% and 50%; this also did not change the results.

A. J., Gorosabel J., Thoene C. C., Dominguez R., 2011, GRB Coordinates Network, 12234, 1
Cano Z. et al., 2009, GRB Coordinates Network, 10066, 1
Cenko S. B., Cucchiara A., Fox D. B., Berger E., Price P. A., 2007a, GRB Coordinates Network, 6888, 1
Cenko S. B. et al., 2010, ApJ, 711, 641
Cenko S. B., Gezari S., Small T., Fox D. B., Chornock R., 2007b, GRB Coordinates Network, 6322, 1
Cenko S. B., Perley D. A., Junkkarinen V., Burbidge M., Diego U. S., Miller K., 2009, GRB Coordinates Network, 9518, 1
Chen H.-W., Helsby J., Shectman S., Thompson I., Crane J., 2009, GRB Coordinates Network, 10038, 1
Chornock R., Berger E., Fox D., 2011, GRB Coordinates Network, 12537, 1
Chornock R., Berger E., Fox D., Levan A. J., Tanvir N. R., Wiersema K., 2010, GRB Coordinates Network, 11164, 1
Chornock R., Li W., Filippenko A. V., 2009a, GRB Coordinates Network, 10075, 1
Chornock R., Perley D. A., Cenko S. B., Bloom J. S., 2009b, GRB Coordinates Network, 9243, 1
Chornock R., Perley D. A., Cenko S. B., Bloom J. S., Cobb B., Prochaska J. X., 2009c, GRB Coordinates Network, 8994, 1
Chornock R., Perley D. A., Cobb B. E., 2009d, GRB Coordinates Network, 10100, 1
Covino S. et al., 2008a, GRB Coordinates Network, 8692, 1
Covino S. et al., 2008b, MNRAS, 388, 347
Cucchiara A. et al., 2011, ApJ, 743, 154
Cucchiara A., Fox D., Tanvir N., 2009, GRB Coordinates Network, 10065, 1
Cucchiara A., Fox D. B., 2008, GRB Coordinates Network, 7654, 1
Cucchiara A., Fox D. B., Cenko S. B., Berger E., 2008, GRB Coordinates Network, 8713, 1

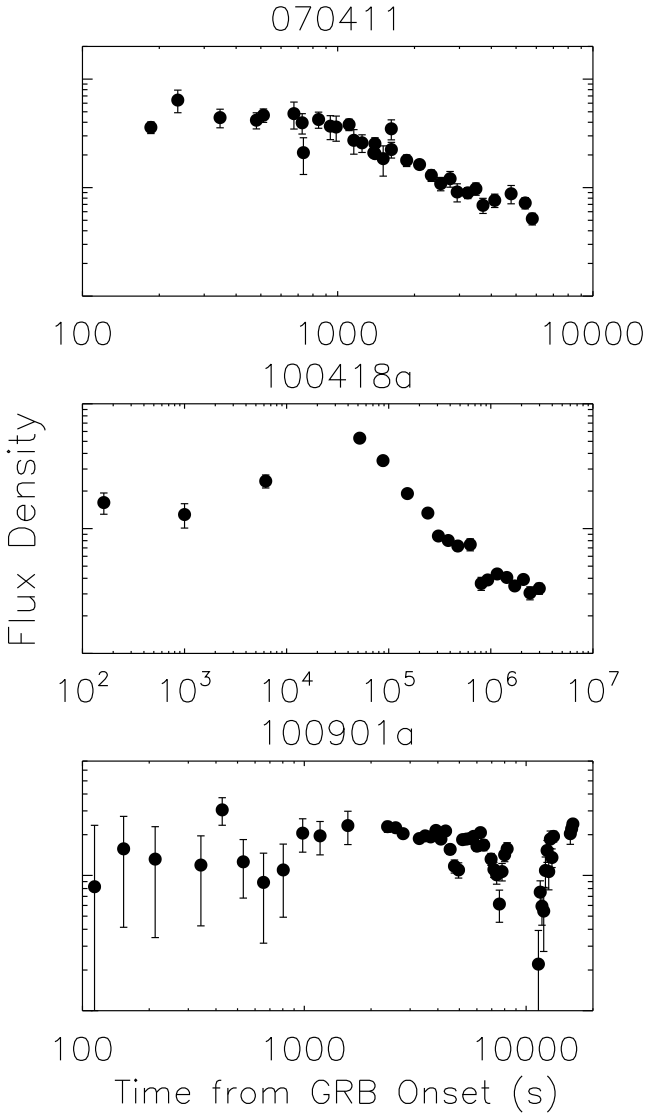

Figure 3. "Difficult to Classify" cases. These neither have a well-defined initial rise and rollover nor an evident initial decay. 070411 is directly adapted from Figure 2 of Ferrero et al. (2008), but does not show the time error bars. These events are treated 3 ways in further analyses: ignored, with the peak set by the end of the rise, and with the peak set by the start of the decay. Further details are in Table 4, which gives the data references.

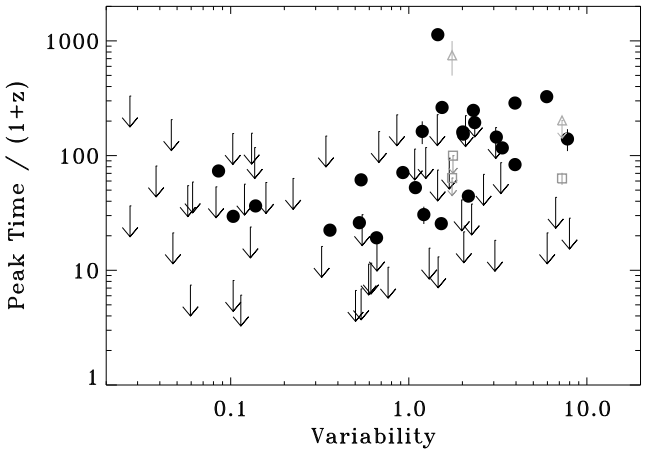

Figure 4. Source frame peak time vs γ-ray variability. Points from Table 3, limits from Table 2. The 3 "hard to classify" cases are included, with points tagged by grey squares for the peak time set by the end of the rise and grey triangles for the time set by the start of the decay. The decay-set peak time of 100418A is off the plot. The detected points suggest a loose positive correlation. It is important to include the peak limits, as they fill in significant parts of the parameter space. The Spearman test (Table 5) indicates that there is no statistical support for a significant correlation between the properties, with a null probability of 2%.

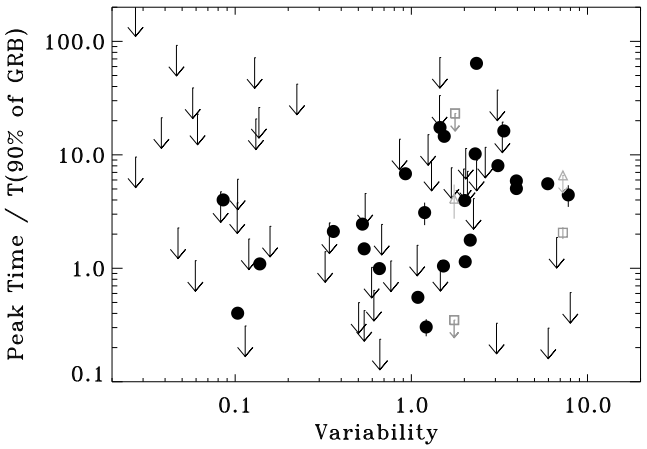

Figure 5. Peak time as a fraction of GRB duration vs γ-ray variability. Points and "hard to classify" cases presented as in Figure 4. The fitted peaks (points) alone also suggest a loose positive correlation, and including the peak limits shows that the results fill in more of the parameter space. The Spearman test (Table 5) indicates that there is no statistical support for a significant correlation between the properties, with a null probability of 2%

Cucchiara A., Price P. A., Fox D. B., Cenko S. B., Schmidt B. P., 2006, GRB Coordinates Network, 5052, 1
Dado S., Dar A., 2009, ArXiv e-prints
D'Avanzo P. et al., 2008, GRB Coordinates Network, 7997, 1
de Pasquale M., Cummings J., 2006, GRB Coordinates Network, 5130, 1
de Pasquale M., Goad M., Blustin A. J., Chester M., Angelini L., Gehrels N., 2005, GRB Coordinates Network, 3960, 1
de Ugarte Postigo A., Castro-Tirado A. J., Tello J. C., Cabrera Lavers A., Reverte D., 2011, GRB Coordinates Network, 11993, 1
de Ugarte Postigo A., Gorosabel J., Fynbo J. P. U., Wiersema K., Tanvir N., 2009a, GRB Coordinates Network, 9771, 1
de Ugarte Postigo A., Jakobsson P., Malesani D., Fynbo J. P. U., Simpson E., Barros S., 2009b, GRB Coordinates Network, 8766, 1
de Ugarte Postigo A., Malesani D., Vreeswijk P. M., Fynbo J. P. U., Jakobsson P., Jaunsen A. O., Sollerman J., 2008, GRB Coordinates Network, 8061, 1
D'Elia V., Covino S., D'Avanzo P., 2008, GRB Coordinates Network, 8438, 1
D'Elia V. et al., 2006, GRB Coordinates Network, 5637, 1
Fatkhullin T. et al., 2009, GRB Coordinates Network, 9712,

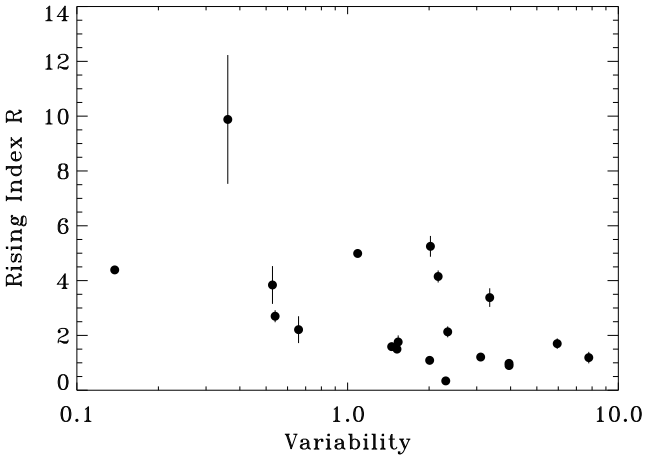

Figure 6. Rising index r vs γ-ray variability V. The indices are from the fit results of Table 3, the asymptotic powerlaw of the fitting shape. Only the 20 events where the formal uncertainty is $< 1/3$ of r are shown. The plot suggests a loose relationship, with a lack of high-r, high-V events. But there is no statistical support for a connection between the properties, with the Spearman test of Table 5 giving a 0.9% null probability and noting that the 20 events is insufficient to trust the accuracy of the test results.

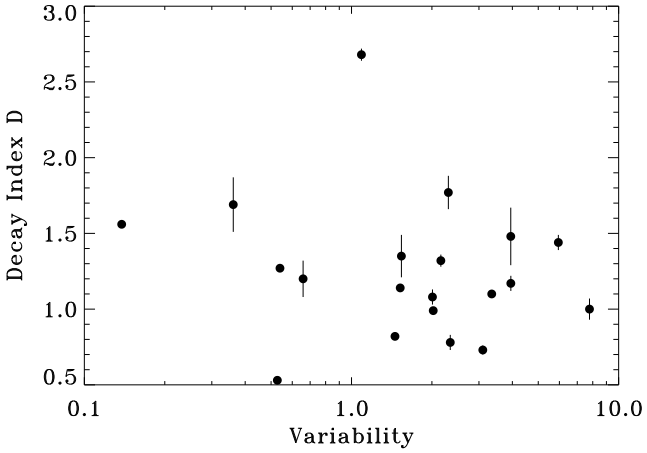

Figure 7. Decaying index d vs γ-ray variability V. The indices are from the fit results of Table 3, the asymptotic powerlaw of the fitting shape. Only the 20 events where the formal uncertainty is $< 1/3$ of d are shown. There is no evidence for a connection between the index and the prompt γ-ray variability.

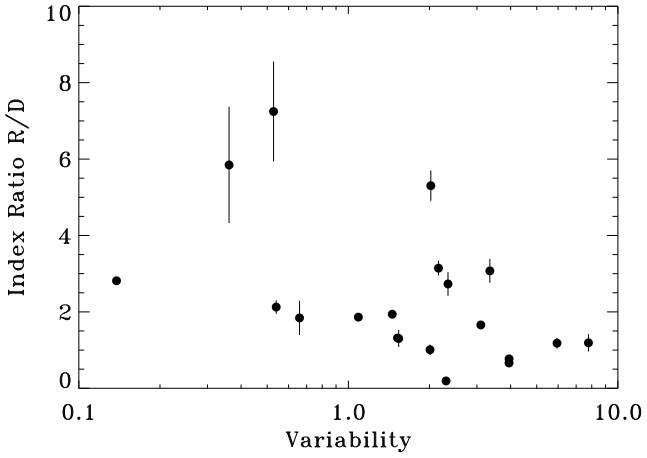

Figure 8. Index ratio r/d (rising / decaying) vs γ-ray variability V. The index ratio is a proxy for the asymmetry in the shape of the optical onset peak. The data suggests a loose relationship, with the dearth in high-ratio, high-V events. But there is no statistical support for a connection between the properties, with the Spearman test of Table 5 giving a null probability of 2% and noting that the 20 events is insufficient to trust the accuracy of the test results.

1
Fatkhullin T. A., Sokolov V. V., Guziy S., de Ugarte Postigo A., Perez-Ramirez D., Gorosabel J., Jelinek M., Castro-Tirado A. J., 2007, GRB Coordinates Network, 6984, 1
Fenimore E. E., Ramirez-Ruiz E., 2000, ArXiv Astrophysics e-prints
Ferrero P. et al., 2008, in American Institute of Physics Conference Series, Vol. 1000, American Institute of Physics Conference Series, Galassi M., Palmer D., Fenimore E., eds., pp. 257–260
Filgas R. et al., 2011, A&A, 526, A113
Fishman G. J., Meegan C. A., 1995, ARA&A, 33, 415
Foley R. J., Chen H.-W., Bloom J., Prochaska J. X., 2005, GRB Coordinates Network, 3483, 1
Fugazza D. et al., 2006, GRB Coordinates Network, 5513, 1
Fugazza D. et al., 2005, GRB Coordinates Network, 3948, 1
Fynbo J., Quirion P.-O., Malesani D., Thoene C. C., Hjorth J., Milvang-Jensen B., Jakobsson P., 2008a, GRB Coordinates Network, 7797, 1
Fynbo J. P. U., Greiner J., Kruehler T., Rossi A., Vreeswijk P., Malesani D., 2008b, GRB Coordinates Network, 8225, 1
Fynbo J. P. U. et al., 2009, Astrophysical Journal Supplement, 185, 526
Fynbo J. P. U., Limousin M., Castro Cerón J. M., Jensen B. L., Naranen J., 2006a, GRB Coordinates Network, 4692, 1
Fynbo J. P. U., Malesani D., Thoene C. C., Vreeswijk P. M., Hjorth J., Henriksen C., 2006b, GRB Coordinates Network, 5809, 1
Fynbo J. P. U. et al., 2005, GRB Coordinates Network, 3749, 1
Fynbo J. P. U., Thoene C. C., Malesani D., Hjorth J., Vreeswijk P. M., Jakobsson P., 2007, GRB Coordinates Network, 6759, 1
Gehrels N., Razzaque S., 2013, Frontiers of Physics
Gorbovskoy E. S. et al., 2013, Astronomy Reports, 57, 233
Gorbovskoy E. S. et al., 2012, MNRAS, 421, 1874
Greiner J. et al., 2009, ApJ, 693, 1912
Gruber D. et al., 2011, A&A, 528, A15
Guidorzi C. et al., 2009a, GRB Coordinates Network, 9677, 1
Guidorzi C. et al., 2009b, A&A, 499, 439
Haislip J. et al., 2010, GRB Coordinates Network, 10494, 1
Henden A., Gross J., Denny B., Terrell D., Cooney W., 2009, GRB Coordinates Network, 10073, 1
Holland S. T. et al., 2011, in American Institute of Physics Conference Series, Vol. 1358, American Institute

of Physics Conference Series, McEnery J. E., Racusin J. L., Gehrels N., eds., pp. 130–133
Jakobsson P., Fynbo J. P. U., Paraficz D., Telting J., Jensen B. L., Hjorth J., Castro Cerón J. M., 2005, GRB Coordinates Network, 4029, 1
Jakobsson P., Fynbo J. P. U., Vreeswijk P. M., de Ugarte Postigo A., 2008a, GRB Coordinates Network, 8077, 1
Jakobsson P., Levan A., Chapman R., Rol E., Tanvir N., Vreeswijk P., Watson D., 2006, GRB Coordinates Network, 5617, 1
Jakobsson P., Malesani D., Thoene C. C., Fynbo J. P. U., Hjorth J., Jaunsen A. O., Andersen M. I., Vreeswijk P. M., 2007, GRB Coordinates Network, 6283, 1
Jakobsson P., Vreeswijk P. M., Malesani D., Jaunsen A. O., Fynbo J. P. U., Hjorth J., Tanvir N. R., 2008b, GRB Coordinates Network, 7286, 1
Jakobsson P., Vreeswijk P. M., Xu D., Thoene C. C., 2008c, GRB Coordinates Network, 7832, 1
Jaunsen A. O., Fynbo J. P. U., Andersen M. I., Vreeswijk P., 2007, GRB Coordinates Network, 6216, 1
Kann D. A., Laux U., Ertel S., 2008, GRB Coordinates Network, 7845, 1
Klotz A., Boer M., Atteia J. L., 2008a, GRB Coordinates Network, 7280, 1
Klotz A., Boer M., Atteia J. L., 2008b, GRB Coordinates Network, 7646, 1
Klotz A., Gendre B., Boer M., Atteia J. L., 2009, GRB Coordinates Network, 8764, 1
Klotz A., Gendre B., Boer M., Atteia J. L., 2012a, GRB Coordinates Network, 13108, 1
Klotz A., Gendre B., Boer M., Atteia J. L., 2012b, GRB Coordinates Network, 13107, 1
Kruehler T., Greiner J., Kann D. A., 2013, GRB Coordinates Network, 14500, 1
Krühler T. et al., 2009a, A&A, 508, 593
Krühler T. et al., 2009b, ApJ, 697, 758
Krushinski V. et al., 2011, GRB Coordinates Network, 12789, 1
Kuin N. P. M. et al., 2009, MNRAS, 395, L21
Kumar P., Zhang B., 2015, Physics Reports, 561, 1
Kuroda D. et al., 2011, GRB Coordinates Network, 12233, 1
Laas-Bourez M., Gendre B., Atteia J. L., Klotz A., Boer M., 2011, GRB Coordinates Network, 11613, 1
Lacluyze A. et al., 2011a, GRB Coordinates Network, 12544, 1
Lacluyze A. et al., 2011b, GRB Coordinates Network, 12535, 1
Lacluyze A. et al., 2009, GRB Coordinates Network, 10107, 1
Landsman W., de Pasquale M., Kuin P., Schady P., Smith P., Parsons A., 2008, GRB Coordinates Network, 8601, 1
Ledoux C., Jakobsson P., Jaunsen A. O., Thoene C. C., Vreeswijk P. M., Malesani D., Fynbo J. P. U., Hjorth J., 2007, GRB Coordinates Network, 7023, 1
Ledoux C. et al., 2005, GRB Coordinates Network, 3860, 1
Ledoux C., Vreeswijk P., Smette A., Jaunsen A., Kaufer A., 2006, GRB Coordinates Network, 5237, 1
Levesque E., Chornock R., Kewley L., Bloom J. S., Prochaska J. X., Perley D. A., Cenko S. B., Modjaz M., 2009, GRB Coordinates Network, 9264, 1
Liang E.-W. et al., 2013, ApJ, 774, 13
Liang E.-W., Yi S.-X., Zhang J., Lü H.-J., Zhang B.-B., Zhang B., 2010, ApJ, 725, 2209
Lipunov V. et al., 2006a, GRB Coordinates Network, 5901, 1
Lipunov V. et al., 2006b, GRB Coordinates Network, 5632, 1
Malesani D. et al., 2011, GRB Coordinates Network, 11977, 1
Malesani D., Fynbo J. P. U., Jakobsson P., Vreeswijk P. M., Niemi S.-M., 2008, GRB Coordinates Network, 7544, 1
Marshall F. E. et al., 2011, ApJ, 727, 132
Maticic S., Skvarc J., 2009, GRB Coordinates Network, 9715, 1
Meehan S., Hanlon L., Topinka M., Kubanek P., 2012, GRB Coordinates Network, 13144, 1
Melandri A., Grazian A., Guidorzi C., Monfardini A., Mundell C. G., Gomboc A., 2006a, GRB Coordinates Network, 4539, 1
Melandri A. et al., 2009, MNRAS, 395, 1941
Melandri A. et al., 2006b, GRB Coordinates Network, 5103, 1
Melandri A. et al., 2010, ApJ, 723, 1331
Melandri A. et al., 2006c, GRB Coordinates Network, 5804, 1
Mészáros P., 2006, Reports on Progress in Physics, 69, 2259
Mészáros P., Gehrels N., 2012, Research in Astronomy and Astrophysics, 12, 1139
Milvang-Jensen B. et al., 2010, GRB Coordinates Network, 10876, 1
Molinari E. et al., 2007, A&A, 469, L13
Monfardini A. et al., 2006, ApJ, 648, 1125
Mundell C. G. et al., 2009, GRB Coordinates Network, 10063, 1
Oates S. R., 2011, GRB Coordinates Network, 12000, 1
Oates S. R. et al., 2007, MNRAS, 380, 270
Oates S. R., Markwardt C. B., Norris J., Evans P. A., Littlejohns O., 2010, GCN Report, 300, 1
Oates S. R. et al., 2006, MNRAS, 372, 327
Oates S. R. et al., 2009, MNRAS, 395, 490
O'Meara J., Chen H.-W., Prochaska J. X., 2010, GRB Coordinates Network, 11089, 1
Osip D., Chen H.-W., Prochaska J. X., 2006, GRB Coordinates Network, 5715, 1
Page K. L. et al., 2009, MNRAS, 400, 134
Panaitescu A., Vestrand W. T., Woźniak P., 2013, MNRAS, 433, 759
Parhomenko A. V. et al., 2011, GRB Coordinates Network, 12238, 1
Perley D. A., Chornock R., Bloom J. S., 2008a, GRB Coordinates Network, 7962, 1
Perley D. A., Chornock R., Bloom J. S., Fassnacht C., Auger M. W., 2007, GRB Coordinates Network, 6850, 1
Perley D. A., Klein C. R., Morgan A. N., Li W., 2010, GRB Coordinates Network, 11007, 1
Perley D. A. et al., 2008b, ApJ, 688, 470
Perley D. A. et al., 2011, AJ, 141, 36
Peterson B., Schmidt B., 2006, GRB Coordinates Network, 5223, 1
Poole T. S., La Parola V., 2006, GRB Coordinates Network, 5068, 1
Price P. A., 2006, GRB Coordinates Network, 5104, 1

Prochaska J. X., 2005, GRB Coordinates Network, 4271, 1
Prochaska J. X., Chen H.-W., Bloom J. S., Falco E., Dupree A. K., 2006, GRB Coordinates Network, 5002, 1
Prochaska J. X., Chen H.-W., Bloom J. S., O'Meara J., Burles S. M., Thompson I., 2005a, GRB Coordinates Network, 3732, 1
Prochaska J. X., Ellison S., Foley R. J., Bloom J. S., Chen H.-W., 2005b, GRB Coordinates Network, 3332, 1
Prochaska J. X., Perley D., Howard A., Chen H.-W., Marcy G., Fischer D., Wilburn C., 2008a, GRB Coordinates Network, 8083, 1
Prochaska J. X., Perley D. A., Modjaz M., Bloom J. S., Poznanski D., Chen H.-W., 2007, GRB Coordinates Network, 6864, 1
Prochaska J. X., Shiode J., Bloom J. S., Perley D. A., Miller A. A., Starr D., Kennedy R., Brewer J., 2008b, GRB Coordinates Network, 7849, 1
Quimby R., Fox D., Hoeflich P., Roman B., Wheeler J. C., 2005, GRB Coordinates Network, 4221, 1
Reichart D. E., Lamb D. Q., Fenimore E. E., Ramirez-Ruiz E., Cline T. L., Hurley K., 2001, ApJ, 552, 57
Roming P. W. A. et al., 2009, ApJ, 690, 163
Rujopakarn W., Guver T., Smith D. A., 2008, GRB Coordinates Network, 7792, 1
Rykoff E. S. et al., 2009, ApJ, 702, 489
Rykoff E. S., Rujopakarn W., 2008, GRB Coordinates Network, 7593, 1
Sanchez-Ramirez R., Gorosabel J., Castro-Tirado A. J., Rivero M. A., Gomez-Velarde G., 2012, GRB Coordinates Network, 13146, 1
Sari R., Piran T., 1999, ApJ, 520, 641
Saxton C., de Pasquale M., Beardmore A., 2010, GCN Report, 303, 1
Schaefer B. E., 2007, ApJ, 660, 16
Schaefer B. E., McKay T. A., Yuan F., 2007, GRB Coordinates Network, 6948, 1
Schulze S., Covino S., Flores H., Fynbo J. P. U., Milvang-Jensen B., Sollerman J., Xu D., 2011, GRB Coordinates Network, 12770, 1
Sokolov V. V., Moskvitin A. S., Fatkhullun T. A., 2011, GRB Coordinates Network, 12241, 1
Sparre M. et al., 2011, GRB Coordinates Network, 11607, 1
Starling R. L. C. et al., 2009, MNRAS, 400, 90
Tanvir N. R. et al., 2010, GRB Coordinates Network, 11123, 1
Tello J. C., Sanchez-Ramirez R., Gorosabel J., Castro-Tirado A. J., Rivero M. A., Gomez-Velarde G., Klotz A., 2012, GRB Coordinates Network, 13118, 1
Thoene C. C., de Ugarte Postigo A., Vreeswijk P. M., Malesani D., Jakobsson P., 2008a, GRB Coordinates Network, 8058, 1
Thoene C. C., Malesani D., Vreeswijk P. M., Fynbo J. P. U., Jakobsson P., Ledoux C., Smette A., 2008b, GRB Coordinates Network, 7602, 1
Updike A., Nicuesa A., Nardini M., Kruehler T., Greiner J., 2010, GRB Coordinates Network, 10874, 1
Updike A. C., Hartmann D. H., Milne P. A., Williams G. G., 2009, GRB Coordinates Network, 10074, 1
Šimon V., Polášek C., Jelínek M., Hudec R., Štrobl J., 2010, A&A, 510, A49
Vergani S. D. et al., 2010, GRB Coordinates Network, 10495, 1
Vreeswijk P. M., Thoene C. C., Malesani D., Fynbo J. P. U., Hjorth J., Jakobsson P., Tanvir N. R., Levan A. J., 2008, GRB Coordinates Network, 7601, 1
Wang Z., Bassa C., Kaspi V. M., Bryant J. J., Morrell N., 2008, ApJ, 679, 1443
Wiersema K. et al., 2012, MNRAS, 426, 2
Wiersema K., Levan A., Kamble A., Tanvir N., Malesani D., 2009, GRB Coordinates Network, 9673, 1
Wiersema K., Tanvir N., Vreeswijk P., Fynbo J., Starling R., Rol E., Jakobsson P., 2008, GRB Coordinates Network, 7517, 1
Wren J., Vestrand W. T., Wozniak P. R., Davis H., 2008, GRB Coordinates Network, 7477, 1
Xiao L., Schaefer B. E., 2009, ApJ, 707, 387
Xin L.-P. et al., 2011, MNRAS, 410, 27
Xin L. P., Zheng W. K., Qiu Y. L., Wei J. Y., Wang J., Deng J. S., Urata Y., Hu J. Y., 2009, GRB Coordinates Network, 9225, 1
Yost S. A. et al., 2006, ApJ, 636, 959
Yost S. A. et al., 2007, ApJ, 657, 925
Yuan F., Rykoff E. S., McKay T. A., Schaefer B. E., Quimby R., Swan H., 2007, GRB Coordinates Network, 6951, 1
Zhai M., Xing L. P., Qiu Y. L., Wei J. Y., Hu J. Y., Deng J. S., Zheng W. K., 2006, GRB Coordinates Network, 5798, 1